PAPER

Molecular dynamics simulations of anisotropic explosions of small hydrogen clusters in intense laser pulses

IOP Publishing Journal of Physics B: Atomic, Molecular and Optical Physics
J. Phys. B: At. Mol. Opt. Phys. **48** (2015) 035601 (8pp) doi:10.1088/0953-4075/48/3/035601

Molecular dynamics simulations of anisotropic explosions of small hydrogen clusters in intense laser pulses

Rong Cheng[1,2], **Chunyan Zhang**[3], **Li-Bin Fu**[1,4] **and Jie Liu**[1,4]

[1] National Laboratory of Science and Technology on Computational Physics, Institute of Applied Physics and Computational Mathematics, Beijing 100088, People's Republic of China
[2] Department of Physics, Teacher Education College, Qingdao University, Qingdao 266071, People's Republic of China
[3] Department of Physics, Hubei University for Nationalities, Eenshi 445000, People's Republic of China
[4] Center for Applied Physics and Technology, Peking University, Beijing 100084, People's Republic of China

E-mail: lbfu@iapcm.an.cn and liu_jie@iapcm.an.cn

Received 25 September 2014, revised 28 November 2014
Accepted for publication 8 December 2014
Published 13 January 2015

Abstract

The explosion dynamics of small hydrogen clusters irradiated by intense femtosecond infrared laser pulses is investigated by classical molecular dynamics simulations. We find a spatial anisotropy in these explosions with proton energies enhanced along the laser polarization direction. Our simulations can identify the origin of this anisotropy: the interplay between the space charge separation in the early stage of cluster ionization and the Coulomb attraction between the rescattered electrons and protons during cluster explosion.

Keywords: molecular dynamics simulation, cluster dynamics, intense laser field

(Some figures may appear in colour only in the online journal)

1. Introduction

Rapid advances of ultrastrong and ultrashort pulse laser sources have opened a new way for the investigation of the interaction of intense laser with atomic clusters, which has attracted considerable attention in recent years. The original advantage combining both gaseous and solid targets allows clusters to provide optimal conditions for such processes as production of energetic electrons and ions [1, 2], incoherent as well as coherent x-ray emission [3, 4], fusion reaction in deuterium clusters [5], high-order harmonic generation [6], etc. To design such experiments, a thorough understanding of the dynamics of laser-cluster interaction is essential.

The interaction process of intense laser pulses with clusters can be simply divided into three subprocesses: inner ionization, outer ionization and expansion of clusters. There are two different models describing these processes, namely, Coulomb explosion and hydrodynamic expansion models depending upon the laser and cluster parameters. In the former, the small clusters promptly have most of their electrons stripped by ultrastrong laser pulses and a uniform positive charged cluster forms. Then the cluster ions explode isotropically through the Coulomb repulsive forces [7]. On the other hand, the hydrodynamic expansion model is suitable for large clusters and modest intensity laser pulses. If the majority of the free electrons are still bound by the space-charge field of the cluster ions, the cluster can be pictured as a quasi-neutral plasma sphere and explodes isotropically due to the electron gas pressure [8, 9]. However, in the intermediate situations, the electrons are neither pulled out of the clusters instantly nor retained bound the clusters permanently, either of these extreme cases will have limited success in describing the cluster dynamics process and explaining some of the observations, such as anisotropic explosion.

Anisotropy has been observed by a number of groups in ion energy spectra measurements from various cluster species and sizes irradiated at modest intensity ($\sim 10^{16}$ W cm^{-2}) [10–15]. When the laser pulse length is comparable to or longer than a typical cluster explosion time (many-cycle regime), more energetic ions are emitted along the laser polarization

direction rather than the perpendicular direction [10–13]. For xenon clusters, it has been explained that the laser-induced surface polarization can lead to preferential acceleration of surface ions along the laser field [10]. For argon clusters, the experimental studies [11, 12], in conjunction with microscopic particle-in-cell (PIC) simulations [16], strongly suggest that the production of higher charge state ions near the poles of the cluster and direct laser field acceleration of these highly charged ions result in the anisotropic explosion with ion energies enhanced along the laser polarization direction. In contrast, with shorter laser pulses available (few-cycle regime), for xenon and argon clusters, the yield of ions is higher along the perpendicular rather along the parallel direction of laser polarization [14, 15]. It can be explained on the basis of screening of the ions by the inner electron cloud inside the cluster [17].

For hydrogen clusters, recent experiments reported a clear spatial anisotropy in the energy spectra of ions ejected from H_2 clusters irradiated at high intensity (nearly 10^{18} W cm^{-2}) [13]. In [13], the observed ion anisotropy was interpreted in light of incomplete stripping of the clusters by the field and the oscillating electron cloud around the cluster, as predicted by the nonlinear theory of [18, 19]. In the nonlinear theory, a characteristic length d_0 representing the space-charge separation displacement inside the cluster is derived for classifying the cluster size and $d_0 = 3F_0/4\pi\rho_0$ (atomic unit) with amplitude of laser field F_0 and initial ion density ρ_0. The ion expansion is assumed to be anisotropic only for medium and large clusters, where the initial cluster radius R_0 is require to be larger than d_0. While the experimental parameters of [13] link the situation of $R_0 < d_0$ and the phenomenon of anisotropic explosion still exists. Therefore, the explosion mechanism of the small hydrogen clusters is unclear and a detailed study of the interaction process of intense laser fields with small hydrogen clusters is highly desired.

In this paper, we investigate the interaction process of intense femtosecond laser pulses with isolated small hydrogen clusters. A three-dimensional molecular dynamics (MD) simulation with the LAMMPS code is introduced to efficiently calculate all individual two-body interactions[6]. Our simulations show the anisotropic explosion of the small hydrogen clusters with the highest energy protons emitting along the laser polarization direction. Moreover, we can identify the origin of this anisotropy that can be attributed to two effects. In the early stage of cluster ionization, the anisotropically space-charge separation inside the clusters dominates this anisotropy. While, during cluster explosion, the anisotropically Coulomb attraction between the rescattered electrons and protons dominates.

The paper is organized as follows. In section 2, we describe the MD simulation model in detail. Section 3 is devoted to analyzing the simulation results. The origin of anisotropy identified by MD simulations is presented and discussed. Finally, a brief summary is given in section 4.

[6] See the LAMMPS WWW Site at http://lammps.sandia.gov.

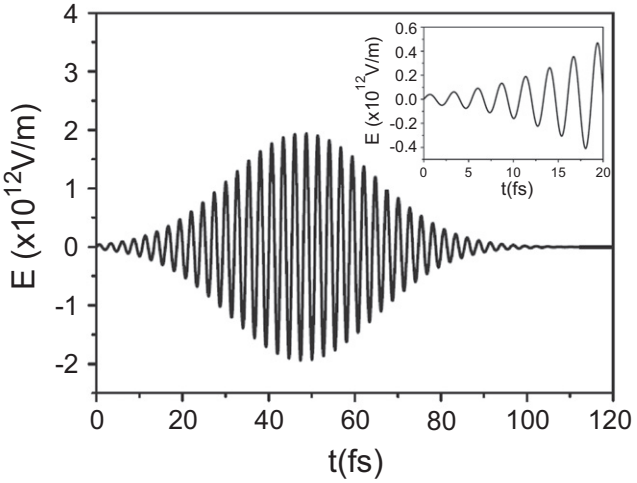

Figure 1. Laser electric field versus time. The insert magnifies the curve between 0 ~ 20 fs.

2. Simulation model

In recent years, a number of MD models have been developed to explore various aspects of laser-cluster interaction [20–25]. These particle models can catch the essential features of cluster dynamics and provide a good description of the clusters, such as the position and velocity distributions of particles. MD simulations have proved to be more suitable for the small clusters than PIC simulations [26–29].

We first formulate our MD model with the relevant parameters as in the experiments of [13], where the laser intensity is so strong that we can neglect the molecular structure of H_2 in MD simulations. These experiments are conducted in the limit of low cluster density, and the impact of neighboring clusters is negligible. Hence we can only consider an isolated hydrogen cluster with open boundary conditions. Initially, the hydrogen cluster is spherically symmetric with the radius $R_0 = 20$ Å and spatially uniform with ion density $\rho_0 = 0.055$ Å^{-3}. In our model, all protons and electrons are initialized by assigning each charge, initial position and velocity. The protons uniformly distribute in a sphere with zero velocities. The initial states of the bound electrons are determined by a microcanonical distribution as in [30], which is distinct from our previous work [25]. The cluster is irradiated by a laser with pulse width $T = 40$ fs, peak intensity $I_0 = 5 \times 10^{17}$ W cm^{-2}, and wavelength $\lambda = 800$ nm. The laser pulse, shown in figure 1, has a shape of Gaussian profile $I(t) = I_0 \exp[-2.773(t - t_0)^2/T^2]$ turned on at time $t = 0$ and approaching its peak at time $t = t_0 = 48$ fs. The laser pulse propagates along the y axis and is linearly polarized in the z direction.

At time $t = 0$, the beginning of the calculation, the cluster is neutral. As time advances, the laser intensity increases, and at appropriate intensity the neutral atoms are ionized through optical field ionization and collisional ionization. Thus, we obtain protons and unbound electrons, and the latter consists of both free electrons that are still bound the cluster (inner ionization electrons) and free electrons that are extracted out

of the cluster (outer ionization electrons). All charged particles are treated classically and advanced according to the Newton equation of motion at each time step:

$$\frac{\mathrm{d}\boldsymbol{p}_i}{\mathrm{d}t} = q_i \boldsymbol{F}_0(t) - \sum_{j\neq i} \nabla \Phi_{ij}, \tag{1}$$

where $\boldsymbol{p}_i$ and q_i are momentum and charge of the ith particle, respectively. $\boldsymbol{F}_0(t)$ is the laser electric field, and Φ_{ij} is the interaction potential between particles i and j. In our calculation, soft Coulomb potential is taken into account to describe the interactions between any two different particles:

$$\Phi_{ij} = \frac{1}{4\pi\varepsilon_0}\frac{q_i q_j}{r_{ij}}, \tag{2a}$$

$$\Phi_{ij} = \frac{1}{4\pi\varepsilon_0}\frac{q_i q_j}{r_{ij}} + \frac{c}{r_{ij}^6}, \tag{2b}$$

where equation (2*a*) represents the interaction potential between homogeneous particles, ε_0 is the vacuum permittivity, r_{ij} is the distance between two particles; equation (2*b*) represents the electron–proton interaction potential, c/r_{ij}^6 is the smoothing term which is introduced to avoid a steep increase in forces at very short distances [31]. For the hydrogen clusters, $c = 0.1\ \mathrm{N}\cdot\mathrm{m}^7$.

3. Simulation results

The MD simulation is performed to study the interaction process of ultrastrong and ultrashort laser pulses with small hydrogen clusters. In this section, we intend to present some essential characteristics of the ionization and explosion dynamics of clusters.

Firstly, the inner and outer ionization of the clusters as well as the cluster explosion can be visualized by taking snapshots of the cluster configuration at different times, which are plotted in figure 2. The computations have been performed in three dimensions, but for convenience the presentation is two-dimensional in the XZ plane [22]. At $t = 0$, all protons (black spot) and electrons (red or grey spot) reside inside the cluster, and the cluster is neutral (figure 2(a)). After the laser pulse is turned on, part of electrons are promptly ionized from their parent nuclei and extracted out of the cluster. The electrons remaining bound the cluster form a core smaller than the proton cloud radius. And the electron core oscillates along the laser polarization direction (figures 2(b) and (c)). As the laser intensity increases, more electrons are removed from the cluster, and the radius of the electron core gradually decreases (figure 2(d)). Figure 2(e) shows at $t = 16$ fs, the number of the remaining electrons is so small that they can no longer form a core. At about 20 fs (~48 fs before the peak intensity) the ultrastrong laser field removes almost all of the electrons from the cluster, which indicates that the cluster ionization finishes (figure 2(f)). As can be seen from figures 2(a)–(f), the full ionization is not instantaneous even for small clusters with high-intensity lasers, and during the ionization process, electrons and protons separate in space. Hence, the spherical symmetry of the space-charge field inside the cluster is broken, which will destroy the symmetry of cluster explosion.

Figure 2 also shows that with the electrons leaving the cluster, the cluster gradually expands. The cluster becomes slightly elongated in the laser polarization direction (z direction), that is to say, the cluster explosion is anisotropic. After the peak of the laser pulse (figure 2(g)), the number of the electrons inside the cluster increases (figure 2(h)). This phenomenon is called recapture [22], which is due to the fact that fast cluster explosion engulfs the outer electrons nearby.

In figure 3, we focus on analyzing the characteristics of the small hydrogen cluster explosion process. Figure 3(a) shows the time evolutions of radii (scaled by the initial cluster radius R_0) of the elongated clusters in three different directions (x, y and z direction). On one hand, one can see that the radius parallel to the laser polarization R_z is always larger than the radii perpendicular to the laser polarization R_x and R_y (R_x and R_y are the same), which indicates that the velocity of cluster explosion along the laser polarization is larger than that perpendicular to laser polarization. Hence, the cluster explosion is spatially anisotropic. On the other hand, in the early stage of cluster ionization (before about 16 fs), the cluster explosion is slow, and after that the cluster explosion becomes fast. Figure 3(b) shows the time evolution of the ratio R_z/R_x, which, in a sense, can reflect the anisotropy sign of the cluster explosions. $R_z/R_x > 1$ corresponds to the anisotropy with larger explosion velocity along the laser polarization direction. One can read from figure 3(b) that the ratio R_z/R_x quickly increases, and reaches a peak (about 16 fs). Then it descends with slight oscillation (20 fs ~ 80 fs), and finally keeps a stable value larger than 1. To sum up, the explosions of the small hydrogen clusters are anisotropic and the explosion velocities are larger along the laser polarization than perpendicular to the laser polarization.

The above phenomena can be understood as the following notation: in the early stage of the laser pulse, the cluster is partially stripped of electrons, and the electrons remaining bound the cluster form a electron core surrounded by a positive proton shell (see figures 2(b)–(d)). The Coulomb repulsive forces between the excess protons of the outer shell give rise to the slow cluster explosion. The MD simulations show that the electron ionization is always along the laser polarization direction (z-direction) prior to other directions. During the ionization process, the space-charge field inside the cluster due to the space-charge separation, is elongated in the laser polarization direction. As a result, the cycle-averaged electric-field forces acting on the protons are anisotropic. The mechanism can be illustrated by depicting the total electric-field forces acting on the protons created by the external laser field and the induced field at two consecutive laser half cycles during cluster ionization, as shown in figure 4. One can see from figure 4(a) that, at 9 fs, the forces along the direction of the laser field are larger, and those along the opposite direction of the laser field and at the equator (perpendicular to the laser polarization direction) due to the shielding effects of the electrons (see figure 2(c)) are very small, even zero. Hence, the protons are accelerated along the direction of the laser

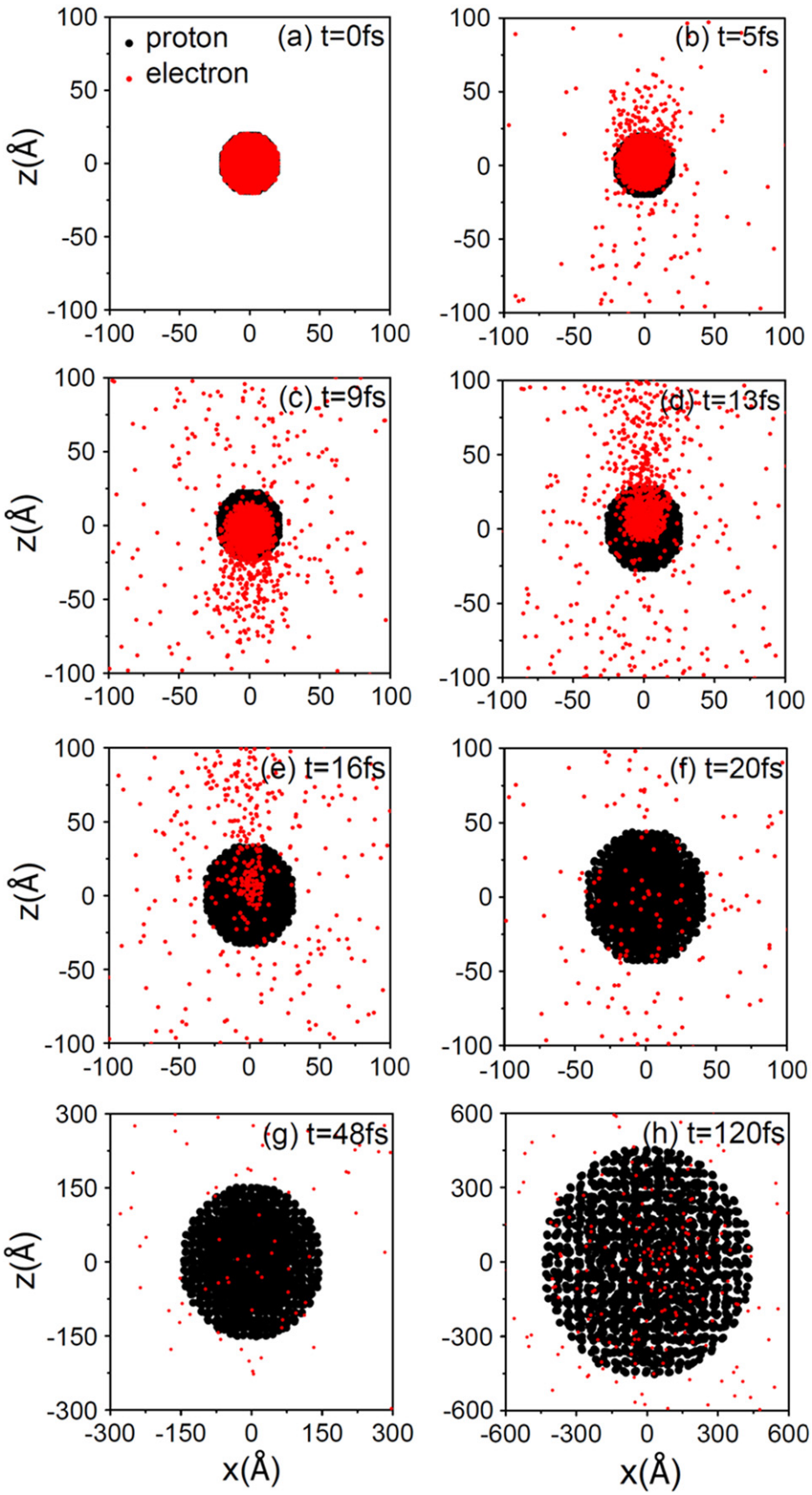

Figure 2. Snapshots of cluster configuration at different times from H_{1850} cluster. Peak laser intensity: $I_0 = 5 \times 10^{17}$ W cm^{-2}, wavelength: $\lambda = 800$ nm, pulse width: $T = 40$ fs, initial cluster radius: $R_0 = 20$ Å and density $\rho_0 = 0.055$ Å^{-3}.

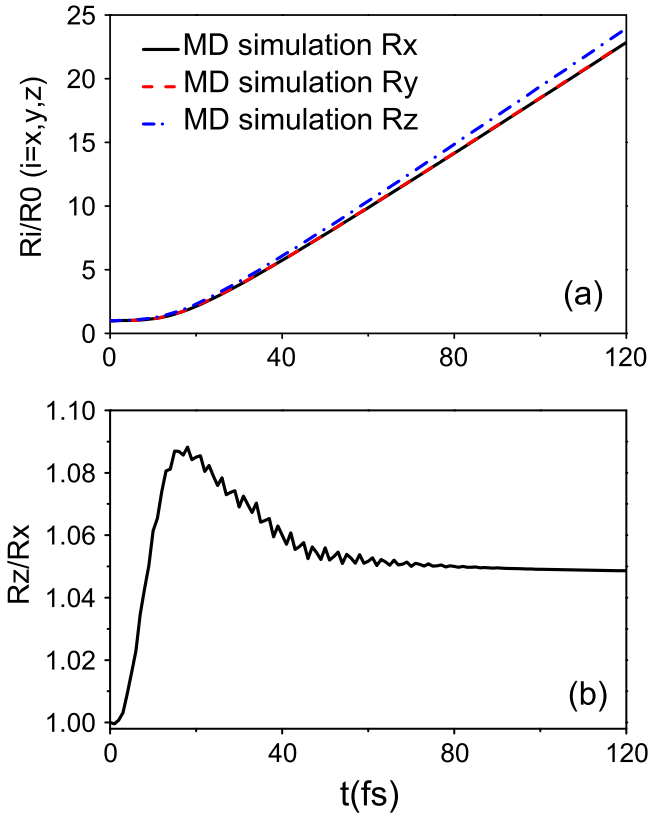

Figure 3. (a) Time evolutions of radii (scaled by the initial cluster radius R_0) of the elongated clusters in three different directions. (b) Time evolution of the ratio R_z/R_x, where R_z is the radius along the laser polarization and R_x is the radius perpendicular to the laser polarization. The parameters are the same as in figure 2.

field prior to other directions. At 10 fs (figure 4(b)), the phase of the laser field reverses, and the forces are still much larger along the direction of the laser field than other directions. The protons are still accelerated along the direction of the laser field prior to other directions. Thus, during cluster ionization, the total electric-field forces acting on the protons, averaged over the laser period, are larger at the poles (parallel to the laser polarization direction) than at the equator. Therefore, the velocities of the protons at the poles are larger. The ratio R_z/R_x quickly increases, and reaches a peak.

After full ionization, almost all of electrons are removed from the clusters (see figures 2(f) and (g)), and no electrons can shield the protons. The protons are accelerated primarily in the electric field of their own space charges. The final kinetic energies of protons are primarily transferred from their initial Coulomb potential energies. Thus the rapid cluster explosion initiates, while the anisotropy caused by the space-charge separation decreases. Meanwhile, as the laser intensity increases, the extracted electrons always oscillate along the laser polarization direction at the laser frequency. They can return to the cluster and be rescattered from it [32]. The mechanism becomes clear by inspecting three typical electron trajectories, numbered (1–3), as shown in figure 5. The left column shows the time evolutions of positions of three typical electrons in x, y and z directions. The oscillations of component z (position in the laser polarization direction) are observed. The time evolutions of corresponding trajectories of the three typical electrons and the average radius of the cluster are shown in the right column. It can be seen, from figures 5(d) and (e), that the trajectories of electron 1 and 2 intersect the cluster radius, respectively. These phenomena imply that the electrons return to the cluster and are rescattered from it before they finally escape from the cluster. The behavior of electron 3 in figure 5(f) exhibit more times rescattering at various points and the phenomenon of recapture, as indicated by the solid arrow, which has been found in figure 2(h). Although the trajectories of the electrons are strongly dependent on their initial positions, all of three typical electrons exhibit oscillation behavior along the laser polarization direction.

During cluster explosion, these rescattered electrons can effectively attract and further accelerate the protons in the laser polarization direction, which ensure the anisotropy sign $R_z/R_x > 1$. After about 80 fs, the distances between protons become long enough that the Coulomb potential energies between them are small. As the laser intensity decreases, the oscillations of the extracted electrons become weaker and weaker. Hence, the value of R_z/R_x finally tends to be stable. Figure 6 shows the electric-field forces acting on the protons by the extracted electrons at two sets of consecutive laser half cycles during cluster explosion. It can be seen that, at 49 fs and 50 fs (figures 6(a) and (b)), the attractive forces acting on the protons are larger in the opposite direction of the laser field than other directions, because the laser field is strong enough to push the extracted electrons to this direction. When the laser field decreases, say, at 100 fs and 101 fs (figures 6(c) and (d)), the electric fields induced by extracted electrons trend to be stable and accumulate at the poles of the clusters. Therefore, during cluster explosion, the cycle-averaged forces are still larger at the poles than at the equator. The protons can gain larger momenta along the laser polarization direction. The cluster explosions are always anisotropic with proton energies enhanced along the laser polarization direction.

Now we pay attention to the energy distribution of the ejected protons from the clusters at the end of the laser pulses. Proton energy spectra calculated for two orthogonal observation angles are shown in figure 7. The angles 0° (solid line) and 90° (dot line) represent observations parallel and perpendicular to the laser polarization direction with an angular cone of $30sr$, respectively. The MD simulation results are the statistical averages of more than 100 sets of data, and the numerical convergence has been tested by increasing the set number of data. The result calculated using pure Coulomb explosion model (dash-dot line) is included for comparison. It is observed that, in the low energy range, the proton energy spectra for parallel and perpendicular to the laser polarization coincide. In the cutoff region, for energies greater than about 1 KeV, the spectra differ. More energetic protons emit along the laser polarization direction (0°). The maximum proton energies are ∼1053 eV at 0° and ∼964 eV at 90°, which are close to the calculated value (∼1.2 KeV) of pure Coulomb explosion model [33]. For small hydrogen clusters, all electrons are extracted in the early stage of the laser pulse. The cluster center undergoes symmetric Coulomb explosion and

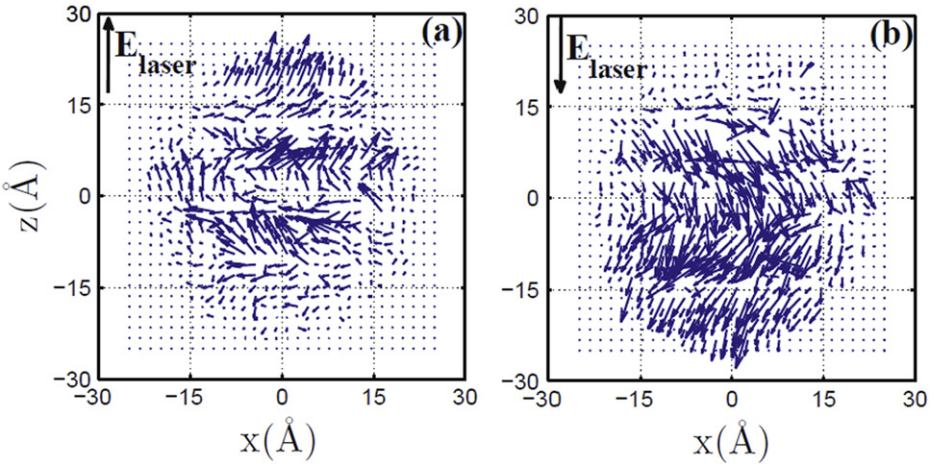

Figure 4. Snapshots of the total electric field forces acting on the protons at the position of the protons at two consecutive laser half cycles: (a) 9 fs and (b) 10 fs. The length and the direction of the arrow represent the magnitude and the direction of the force, respectively. The parameters are the same as in figure 2.

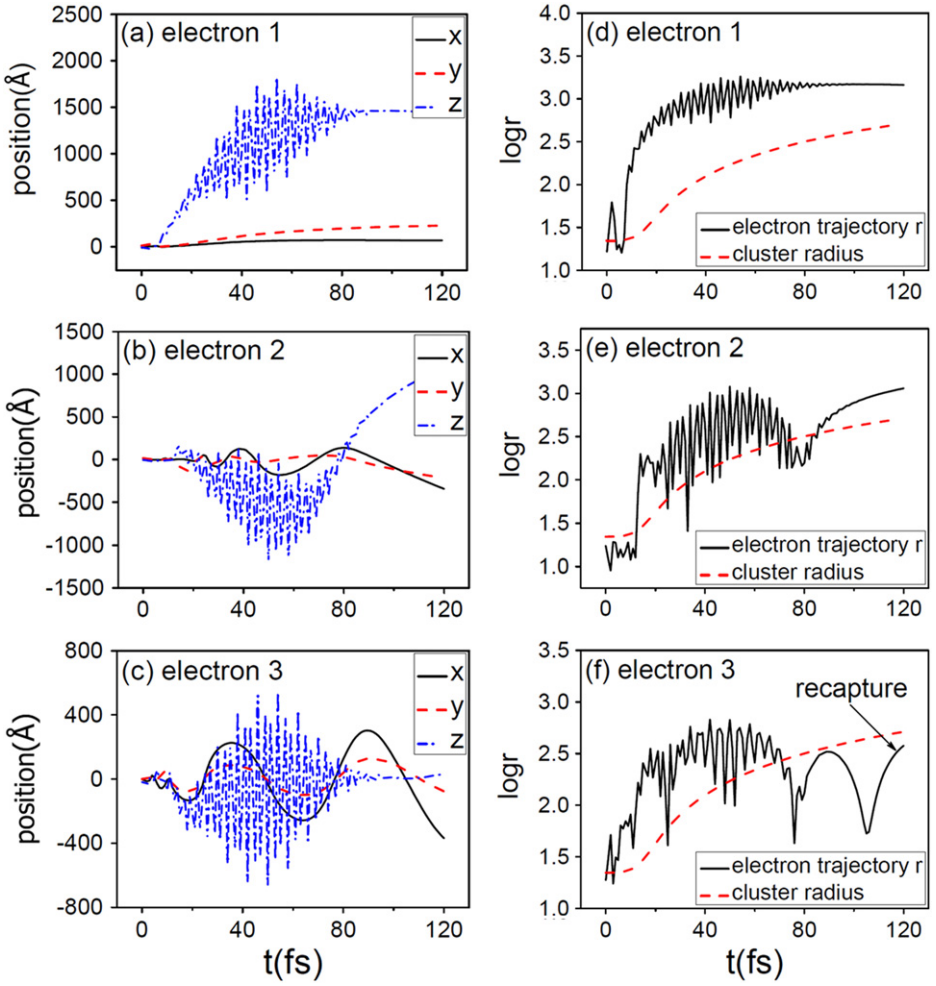

Figure 5. The left column: time evolutions of positions of three typical electrons in x, y and z directions. The right column: time evolutions of trajectories of three typical electrons and the average radius of the cluster. The electron trajectories are given in a logarithmic scale. The parameters are the same as in figure 2.

forms the low energy part of the proton spectra. Those higher energy protons come from near the surface of the clusters. The difference in the cutoff energy of proton spectra indicates that the cycle-averaged accelerating field at the cluster edge is higher along the laser polarization, which is consistent with our analyses in figures 2–6.

At last, we calculate the experiments reporting the anisotropic explosions of hydrogen clusters [13]. Figure 8 shows

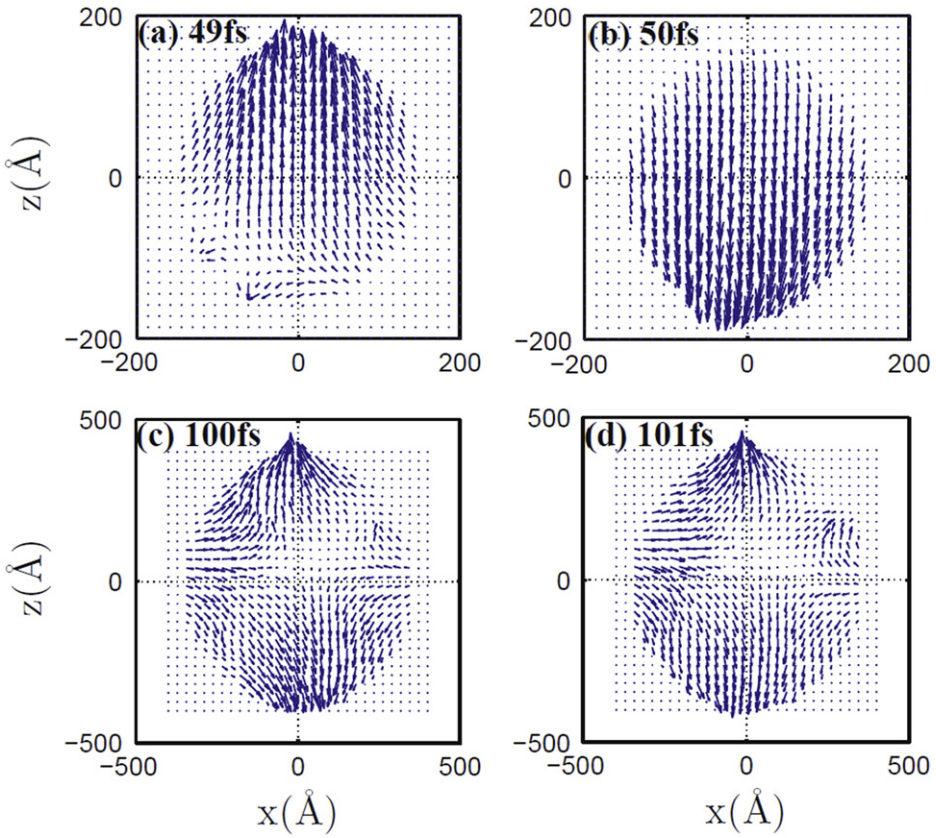

Figure 6. Snapshots of the electric field forces acting on the protons by the extracted electrons at the position of the protons at 49 fs (a); 50 fs (b); 100 fs (c) and 101 fs (d). The length and the direction of the arrow represent the magnitude and the direction of the force, respectively. The parameters are the same as in figure 2.

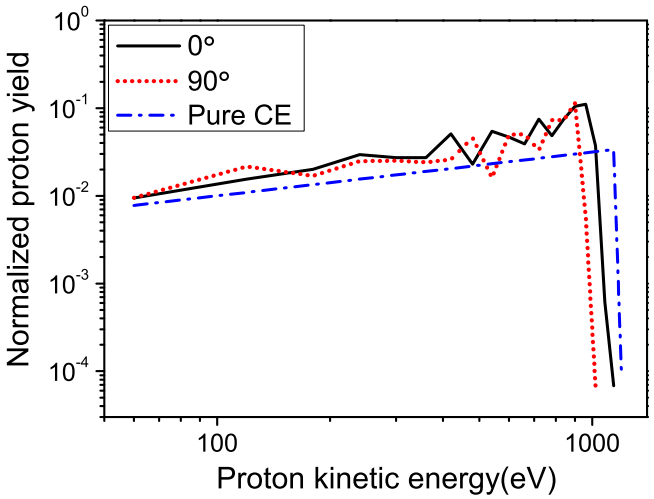

Figure 7. Energy distributions of protons calculated for two orthogonal observation direction, 0° (solid line) and 90° (dot line), where 0° represents observation along the polarization direction of the laser electric field with an angular cone of $30sr$. The dash-dot line is the result calculated using pure Coulomb explosion model. The parameters are the same as in figure 2.

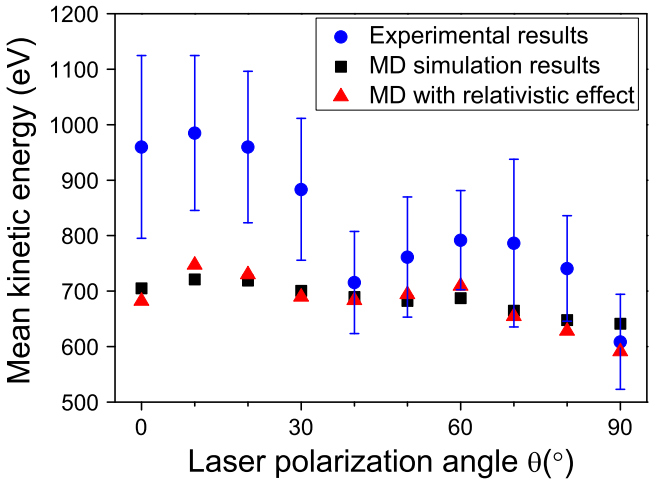

Figure 8. Mean kinetic energies of protons as a function of observation angle where 0° represents observation along the polarization direction of the laser electric field with an angular cone of $10sr$. The (blue) circles: experimental results of [13]. The (black) squares and (red) triangles: MD simulation and MD simulation with relativistic effects results, respectively. The parameters are the same as in figure 2.

our calculation on the mean kinetic energies of protons E_{av} as a function of observation angle θ, where θ is defined as the angle between observation direction and the laser polarization direction. The experimental data of [13] is included for comparison. The MD simulations count the protons ejected along the observation direction in an angular cone of $10sr$. The MD simulation results are the statistical average of more than 100 sets of data and numerical convergence has been

tested by increasing the number of sets of data. Clearly, our simulation results agree with experimental results of [13], especially in the observation angle range of 40° to 90°. In our simulations $E_{av} \approx 705$ eV at 0° while $E_{av} \approx 640$ eV at 90°. Moreover, the degree of anisotropy $\gamma = \left[E_{av}(0°) - E_{av}(90°)\right]/E_{av}(0°) \approx 10\%$, which is lower than the experiment value of ~40%, but it still indicates the anisotropy with more energetic protons emitting along the laser polarization direction, which is the key point of the experiments. The differences can arise from the effects of cluster size and shape distributions as well as the laser pulse duration and intensity distributions, which are not included in our single cluster simulations.

In addition, we carry out relativistic MD simulations. The trajectories of the protons and electrons are governed by the relativistic equations of motion. As can be seen from figure 8, the relativistic effects improve the angular dependence of proton energy slightly. This indicates that, at laser intensity below 10^{18} W cm^{-2}, the laser magnetic field and the induced magnetic field are so small that they cannot affect proton explosion obviously. The relativistic effects are not principal for the present case.

4. Conclusion

In conclusion, by virtue of a three-dimensional MD simulation, we have investigated the interaction process of 20 Å hydrogen cluster with 40 fs, 800 nm laser pulse at peak intensity of 5×10^{17} W cm^{-2}. The ionization and explosion dynamics of the small hydrogen clusters are explored in detail. Our simulations reveal that the cluster explosions are spatially anisotropic with proton energies enhanced along the laser polarization. Then, we show that this anisotropy can be explained as a consequence of two effects: the space charge separation inside the clusters in the early stage of cluster ionization and the Coulomb attraction between the rescattered electrons and protons during cluster explosion. The rescattering effect is an interesting issue and can contribute importantly to the electron dynamics of laser-cluster interactions [32], which deserves a detailed study in the future.

Acknowledgments

This work is supported by the National Fundamental Research Program of China (Contact Nos. 2013CBA01502, 2011CB921503, and 2013CB834100), the National Natural Science Foundation of China (Contact Nos. 11374040 and 11274051).

References

[1] Ditmire T, Tisch J W G, Springate E, Mason M B, Hay N, Smith R A, Marangos J and Hutchinson M H R 1997 *Nature* **386** 54
[2] Gnodtke C, Saalmann U and Rost J M 2012 *Phy. Rev. Lett.* **108** 175003
[3] Ditmire T, Smith R A, Marjoribanks R S, Kulcsar G and Hutchinson M H R 1997 *Appl. Phys. Lett.* **71** 166
[4] Parra E, Alexeev I, Fan J, Kim K Y, McNaught S J and Milchberg H M 2000 *Phy. Rev.* E **62** R5931
[5] Zweiback J, Cowan T E, Smith R A, Hartley J H, Howell R, Steinke C A, Hays G, Wharton K B, Crane J K and Ditmire T 2000 *Phy. Rev. Lett.* **85** 3640
[6] Donnelly T D, Ditmire T, Neuman K, Perry M D and Falcone R W 1996 *Phy. Rev. Lett.* **76** 2472
[7] Last I and Jortner J 2004 *J. Chem. Phys.* **121** 3030
[8] Ditmire T, Donnelly T, Rubenchik A M, Falcone R W and Perry M D 1996 *Phys. Rev.* A **53** 3379
[9] Milchberg H M, McNaught S J and Parra E 2001 *Phys. Rev.* E **64** 056402
[10] Kumarappan V, Krishnamurthy M and Mathur D 2002 *Phys. Rev.* A **66** 033203
[11] Kumarappan V, Krishnamurthy M and Mathur D 2001 *Phys. Rev. Lett.* **87** 085005
[12] Krishnamurthy M, Mathur D and Kumarappan V 2004 *Phys. Rev. A* **69** 033202
[13] Symes D R, Hohenberger M, Henig A and Ditmire T 2007 *Phys. Rev. Lett.* **98** 123401
[14] Skopalova E, El-Taha Y C, Zaïr A, Hohenberger M, Springate E, Tisch J W G, Smith R A and Marangos J P 2010 *Phys. Rev. Lett.* **104** 203401
[15] Mathur D, Rajgara F A, Holkundkar A R and Gupta N K 2010 *Phys. Rev.* A **82** 025201
[16] Jungreuthmayer C, Geissler M, Zanghellini J and Brabec T 2004 *Phys. Rev. Lett.* **92** 133401
[17] Mishra G and Gupta N K 2011 *Eur. Phys. Lett.* **96** 63001
[18] Breizman B N and Arefiev A V 2003 *Plasma Phys. Rep.* **29** 593
[19] Breizman B N, Arefiev A V and Fomyts'kyi M V 2005 *Phys. Plasmas* **12** 056706
[20] Last I and Jortner J 2004 *J. Chem. Phys.* **120** 1336
Last I and Jortner J 2004 *J. Chem. Phys.* **120** 1348
[21] Petrov G M, Davis J, Velikovich A L, Kepple P C, Dasgupta A, Clark R W, Borisov A B, Boyer K and Rhodes C K 2005 *Phys. Rev.* E **71** 036411
[22] Petrov G M, Davis J, Velikovich A L, Kepple P, Dasgupta A and Clark R W 2005 *Phys. Plasmas* **12** 063103
[23] Holkundkar A R, Mishra G and Gupta N K 2011 *Phys. Plasmas* **18** 053102
[24] Mishra G and Gupta N K 2012 *Phys. Plasmas* **19** 093107
[25] Zhang C Y, Zhao Q, Fu L B and Liu J 2012 *Acta Phys. Sin.* **61** 143601 in Chinese
[26] Rose-Petruck C, Schafer K J, Wilson K R and Barty C P J 1997 *Phys. Rev.* A **55** 1182
[27] Junkei K *et al* 2000 *J. Chem. Phys.* **112** 5012
[28] Siedschlag C and Rost J M 2002 *Phys. Rev. Lett.* **89** 173401
[29] Ishikawa K and Blenski T 2000 *Phys. Rev.* A **62** 063204
[30] Abrines R and Percival I C 1996 *Proc. Phys. Soc. London* **88** 861
Leopold J G and Percival I C 1979 *J. Phys. B: At Mol. Phys.* **12** 709
[31] Last I and Jortner J 2000 *Phys. Rev.* A **62** 013201
[32] Saalmann U and Rost J M 2008 *Phys. Rev. Lett.* **100** 133006
[33] Li H Y, Liu J S, Wang C, Ni G Q, Li R X and Xu Z Z 2006 *Phys. Rev.* A **74** 023201